

The glycolytic cycle in yeast cells has often been proposed as an ideal laboratory for the study of dissipative structures in living organisms. In particular metabolic oscillations in yeast cells appear to be a relevant tool for the investigation of control and feedback mechanisms at work in living organisms [6,7]. Here we have chosen to measure the CO_2 production which appears to be a direct and non-invasive way of following the cell metabolic activity, controlling the cell energetic status and the response to external conditions and perturbations. In the present study such perturbations have been induced by changes in the feeding conditions (type of sugar) and/or by soft X-ray irradiation.

The irradiation of *Saccharomyces cerevisiae* cells was carried out with soft X-rays produced with the laser-plasma source at the Rutherford Appleton Laboratory (RAL) [8]. The main idea was to use very soft X-rays in order to produce selective damages to the cell structures (specifically to the cell wall, responsible for part of the metabolic activity, in particular fermentation), avoiding interference with respiration (taking place in mitochondria) and with nuclear and DNA activity. For this purpose, Teflon (CF_2) stripes were chosen as target; when irradiated with high intensity UV laser radiation, they turn into a plasma of C and F He and H like ions. X-rays are emitted from F ions with a K -shell spectrum centred around 0.9 keV. Such X-rays are characterised by a very large absorption in biological matter. X-ray doses to the different cell regions were calculated following a Lambert-Bouguet-Beer law through a spherical model of the cell with concentric and differentiated compartments. The structure of yeast, characterised by a large and massive cell wall [9, 10], contributes to stop most of X-rays before they reach the nucleus, supporting the idea of inducing differential damages. The short penetration depth of the used X-rays and the dosimetric calculation allow to deduce that the main effect is on the metabolic processes in the surface compartments of the cell.

The analysis starts immediately after irradiation and can be continued up to several hours. CO_2 production was monitored by pressure silicon detectors with both irradiated and non irradiated samples.

Preliminary results gave an evidence of reduction in production of the gas for all irradiated samples and of a non-linear cellular response to irradiation dose. Metabolic oscillations in yeast cell suspensions were also observed and it was shown that soft X-ray irradiation at given doses changed the oscillation period. Our results may also allow the development of a non-invasive on-line technique for monitoring the metabolism in cells since the oscillations of the enzymatic cycle and its regulatory mechanisms have been studied with a physical probe, which is active on many cells, and can give quantitative information in a continuous way.

2 Characterisation of yeast cells

A preliminary requirement of the experiment was a precise characterisation of the morphological structure of *Saccha-*

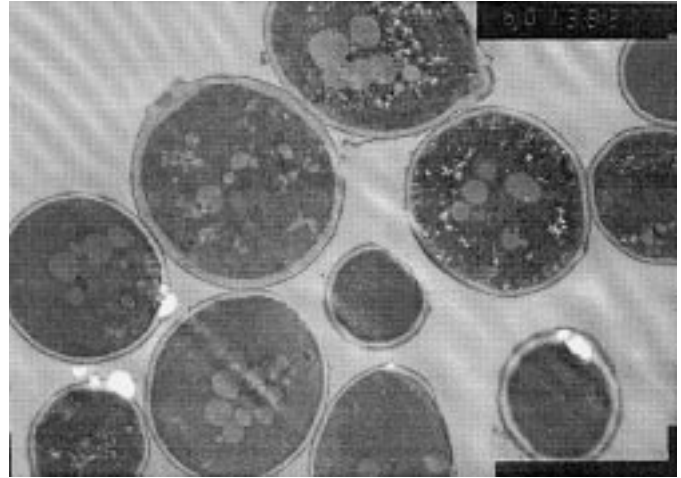


Fig. 2. Picture of yeast cells obtained with TEM at $\times 6000$ magnification.

romyces cerevisiae cells for evaluating the doses in the different cell compartments. For this purpose, cells have been analysed with transmission electron microscopy (TEM).

Figure 2 shows a picture of yeast cells obtained with a $\times 6000$ magnification. It is clearly possible to see the cell nucleus and some vacuoles. The samples were initially hydrated in sterile distilled water for 5 to 6 hours at room temperature until they were starting reproducing by budding. In a second time, being centrifuged for 10 minutes at 3000 g, cells were fixed with 5% glutaraldehyde in 0.1 cacodilate buffer (0.1 M pH 7.2) for two hours. After several washes in the same buffer, yeast cells were postfixed in cacodilate buffer 1% osmium tetroxid, prestained in 1% uranyl acetate in 25% ethanol, dehydrated in a graded ethanol series and embedded in a Epon 812-araldite mixture. Thin sections were obtained with Reichert Ultracurt E ultramicrotome, stained with lead citrate, carbon coated and observed with a Joel 100 SX electron microscope.

The following quantities were measured: cell average radius r_0 ; total membrane and wall thickness S ; nucleus radius r_n together with their distribution; obtaining the values: $r_0 = (2.58 \pm 0.54) \mu\text{m}$; $S = (0.18 \pm 0.02) \mu\text{m}$; $r_n = (0.95 \pm 0.12) \mu\text{m}$.

Concerning cell radius, our values are not too different from those already found in literature [11,12]. Reference [11] also reports measurement of the distribution of yeast cells according to cell radius. This seems to follow a log-normal distribution. As for nuclear radius and wall thickness we did not find sufficient information in literature for our particular yeast strain, which is the main justification of this initial characterisation work.

3 Experimental set-up and procedure

The experimental technique is based on: (i) the utilisation of pressure sensors as a diagnostic toll which allows to monitor cell metabolic response through CO_2 production; and (ii) the use of soft X-rays from a laser-plasma source.

3.1 Preparation of the biological samples

The biological samples were commercial dry *Saccharomyces cerevisiae* Hansen yeast cells (produced by Aboca) that needed to be hydrated about one hour before use. The analysed samples were made by fixed volumes (4 ml) of a suspension of cells in deionized water (or phosphate buffer). Typical concentration of cells was 2 mg/ml corresponding to about 2×10^7 cells/ml. They were filtered in a Venturi tube so that the cells were deposited on a paper filter in a monolayer. After a short period for drying, the filters were put onto a Hostaphan film so that yeast cells were hosted by a “sandwich” made of Hostaphan on one side and paper filter on the other. For the samples undergoing irradiation, such sandwiches were then deposited into an automatic robot for X-ray exposure (the Hostaphan film facing the X-ray source in order to filter unwanted X-rays, *i.e.* those in the water window emitted by Carbon ions, (*cf.* Sect. 3.4) and the dose could be delivered. Finally the filters were put again in the same quantity of water (4 ml) and the bottles were sealed and submerged in a thermal bath at 32 °C (temperature variations were lower than 0.1 °C). Different kinds of sugar were added to the suspension as nourishment in order to study the different metabolic responses. The standard sugar concentration was 20 mg/ml.

Some intermediate investigations were performed, including the optimisation of the support of the biological target (trying different paper filters and different preparation procedures). We also verified that CO₂ production from simple cell suspensions was equivalent to that of sample deposited on the paper filters. During some experimental runs an Argon atmosphere was used, instead of air normally present in the bottle, in order to realise more strict anaerobic conditions and cause a complete inhibition of respiration.

3.2 Gas production measurement

The bottles were connected to the pressure sensors whose output is linked to a PC through an Amplicon 16-20 K sample/s data acquisition board. The pressure sensors were connected to a stabilised 10 V power supply. We used differential silicon pressure sensors (Low Pressure Sensor type AM5310 DV from Miteco) of high sensitivity (from 0 to 100 mbar, giving 25 mV full scale output, with an estimated accuracy of 0.1 mV and a sensitivity of about 2.5 mbar/mV). The sensors were calibrated, showing a very good linearity in the region of interest, and no hysteresis was observed [13]. The data acquisition board has a resolution less than 0.0015 mV.

Before analysing the data, we verified that for control samples (pure water) the pressure measurements perfectly reflected the atmospheric pressure behaviour. Also, in order to be sure that the pressure increase was really due to CO₂ production, mass spectrometry was used (*cf.* Fig. 3).

The acquisition system allowed the simultaneous recording of data from 16 different sample bottles. In

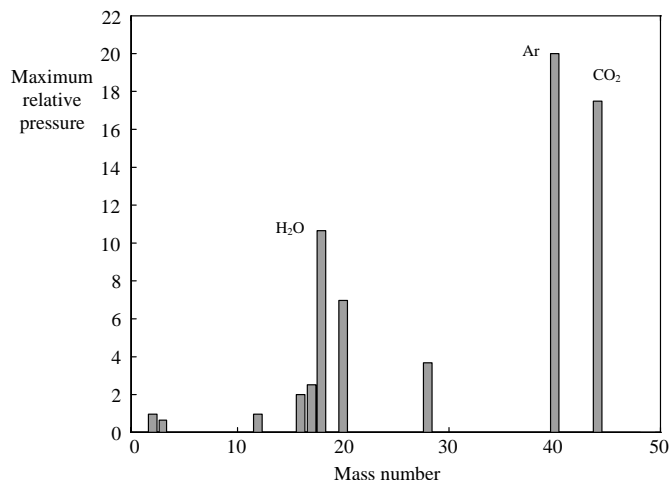


Fig. 3. Mass spectrometry of produced gas as a function of mass number. The initial atmosphere was Argon only, corresponding to anaerobic conditions.

order to check data reproducibility we always had different runs for the same suspension parameters.

3.3 Metabolic modifications induced by soft X-rays

By carefully choosing X-ray wavelength it is conceivable to realise a preferential energy deposition in the cell wall and cytoplasm, where glycolysis and fermentation take place [4], with little interference with mitochondrial and nuclear activity. Even if a marginal damage cannot be excluded for such cell compartments, the calculation of dose distribution (*cf.* Sect. 5) and the results of the experiment are encouraging and suggesting indeed that the main damage is at the metabolic level.

For this purpose the X-ray spectral region which can be used is quite narrow. It was known that X-rays with $h\nu \approx 1.2$ keV, already used for DNA recovery experiments, are characterised by a large penetration depth in undifferentiated biological material ($\approx 5 \mu\text{m}$) and hence can deposit a large quantity of their energy into the cell nucleus [14]. On the other side, the attenuation coefficient is also low for X-rays in the “water window” region (≈ 300 -500 eV) which should then be avoided (*cf.* Fig. 4).

The target material should then be chosen in order to give emission at energies as close as possible to the end of water window (corresponding to the *O*-absorption edge). Also a *K*-shell spectrum, characterised by only a few lines, would be preferable, making the dose calculations much easier. Unfortunately there are not many elements with these characteristics. We chose Fluorine, or rather Teflon (CF₂), which was produced in thin stripes (100 μm thick). The use of stripes drastically reduce the emission of debris which could damage the optics and/or the biological samples [15]. Unfortunately, CF₂ tapes also contain Carbon which exactly emits in the water window. In the present experiment, such undesired *K*-shell C-emission has been removed by putting appropriate filters (2 μm mylar plus 0.2 μm Al) before the biological samples; these filters also

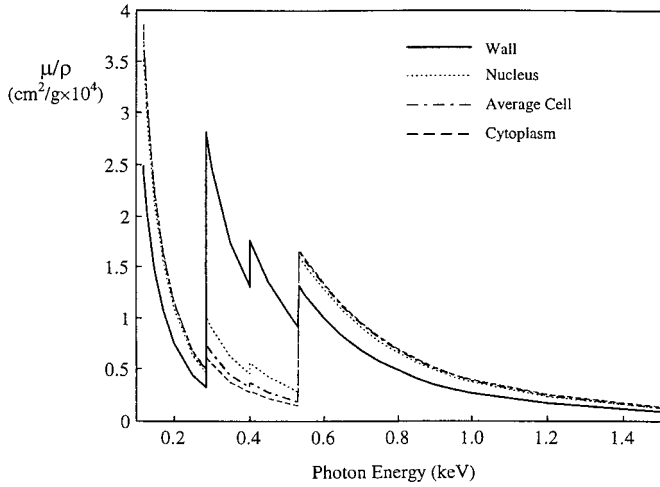


Fig. 4. Mass absorption coefficient of biological material (wall) and biological material with various percentages of water (corresponding to cytoplasm, nucleus, average cell) vs. photon energy in keV.

removed scattered UV laser light, which could be able to produce important biological effects. An additional gas buffer (He at 1 atmosphere) was present in the interaction chamber with the main role of further reducing debris effects, but also contributing to stop the much softer Carbon emission.

3.4 Radiation source

The radiation source was obtained with a complex laser system. A Nd laser, converted to 2ω , was used to pump a dye oscillator followed by dye amplifiers (pumped by an excimer laser) and by frequency converter crystals. The laser pulse so obtained was transformed by spatial and temporal multiplexing in a train of pulses (each 7 pulses long), which underwent a final large amplification in KrF amplifiers, producing UV radiation at $\lambda = 248$ nm. Such laser radiation was focused onto the target with a $f = 9$ cm focusing lens producing an intensity of the order of 5×10^{15} W/cm². The overall system is very similar to the one already described in [8].

A relevant element for the success of the experiment was the availability of a computer driven robot for sample exposure and of a dose control system. The exposure robot has been previously realised at Rutherford Appleton Laboratory in order to irradiate mammal cells with Cu *L*-shell X-rays [14].

The dose control system was based on a silicon PIN diode which measured the X-ray energy produced by each pulse. The PIN was just beside the cell samples and had the same filters placed before the cells in order to exactly measure the same radiation which biological samples were exposed to. Since a single laser shot was in general not enough to give the required dose, successive PIN signals were integrated and summed until the required dose was delivered. The computer then automatically stopped the

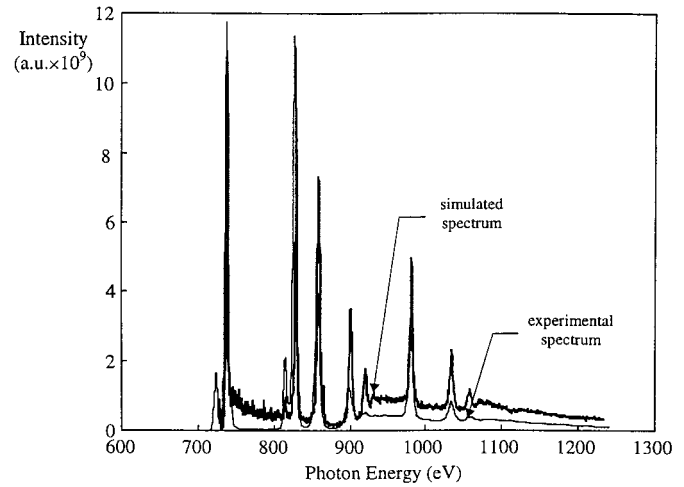


Fig. 5. Comparison between the experimental spectrum and a simulation obtained with the code Ration.

laser, also giving the number of laser shots and the histogram of the dose distribution. In a few minutes the irradiation procedure was completed.

The soft X-ray spectrum was also registered (*cf.* Sect. 4) which allows an absolute calibration of the PIN diode response. The conversion factor used to transform the integrated PIN diode signal (corresponding to a collected electrical charge in nC) to an absorbed dose in rad was 2.6 rad/nC @ 0.9 keV. This is dependent on photon energy because of the variation of PIN sensitivity and the different photon penetration into the biological material.

4 Spectral characteristics of the soft X-ray source

In the observed wavelength range, the X-ray spectrum is a Fluorine *K*-shell one (comprised between the fluorine He- α at 731 eV and the ionisation edge for the H-like ion at 1103 eV). The spectra were recorded with flat crystal minispectrometers (described in [16]) using RbAP crystals ($2d = 26.121$ Å) and Kodak DEF film and filtered with 2 μ m mylar and a 0.2 μ m Al. While recording some spectra, a Cu layer was also added on half the slit: since Cu is characterised by the *L*-absorption edge at $h\nu \approx 0.993$ keV, this gave a wavelength fiducial on the film, which was useful for spectra interpretation. Densitometries of the spectra were obtained with a Joyce Loebel 3CS Microdensitometer at RAL. Absolute X-ray intensities were calculated taking into account film sensitivity [17], filter and buffer gas transparency [18], and crystal reflectivity [19].

Figure 5 shows a comparison between our experimental Fluorine spectrum and the theoretical spectrum produced with the code Ration [20]. The theoretical spectrum has been obtained using a temperature $T_e = 140$ eV and an electron density $n_e = 2 \times 10^{22}$ cm⁻³. A level of 30% Carbon “impurities” (corresponding to the chemical

composition CF₂) and a plasma size of about 10⁻³ cm (roughly the dimension of our laser focal spot) were also used.

It is worth noting that, as expected, the electron density is of the order of the critical density for KrF laser radiation ($n_e = 1.6 \times 10^{22} \text{ cm}^{-3}$), and the temperature value corresponds to the one experimentally measured in our spectrum through the bremsstrahlung slope.

Despite of considerable agreement, care should be taken in considering the results of the simulations. Indeed, while the experimental emission spectrum is the result of temporal changes in the plasma temperature and density profiles, the result obtained with Ration corresponds to a static and uniform plasma with the chosen parameters. A full simulation of the experimental spectrum should imply the coupling to a hydrodynamic code which is anyway clearly beyond the scope of the present work. A more detailed theoretical analysis of our Teflon experimental spectrum has been performed by Magunov *et al.* [21]. Here, the main purpose of the simulations was to give an approximate characterisation of the plasma source in order to deduce “average” plasma parameters which have then been used to obtain a simulated complete CF₂ spectrum containing also Carbon emission, which could not be recorded experimentally. This procedure was performed in order to verify that the filters used between the source and the sample were really useful to cut any radiation emitted in the water window region.

5 Dosimetry

The information obtained from cell characterisation and the careful analysis of the X-ray spectrum allow the development of a detailed spherical model of the cell in order to evaluate the energy absorbed by the micro-organism.

This model allows to calculate separately the doses in the main cell compartments (wall, cytoplasm, nucleus, considered spherical and concentric) and to draw a picture of where X-rays are absorbed and hence of where radiation effects are more likely to occur. This is a clear progress with respect to the approach normally used in radiobiology (*cf.* for instance Ref. [11]) in which only the radiation penetration depth in the undifferentiated biological material and the average dose to the whole cell are considered (in our case, $h\nu \approx 0.9 \text{ keV}$, the penetration depth in an undifferentiated average cell, made of 90% water, is about 1.86 μm).

The absorption coefficients and densities of the three cell compartments are computed according to the following rationale:

- (i) the wall is made of undifferentiated biological material (with no water) with 7% hydrogen, 22.5% oxygen, 52% carbon, 16.5% nitrogen, 1.5% sulphur in weight (as deduced from Ref. [22]), with a density $\rho = 1.6118 \text{ g/cm}^3$;
- (ii) the cytoplasm is composed by 95% water and 5% biological material;

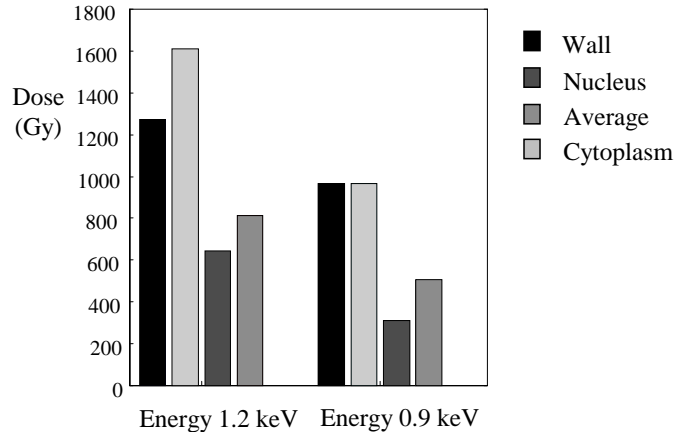


Fig. 6. Results of cell dosimetry for two values of X-ray energy ($h\nu \approx 0.9$ and 1.2 keV) and with wall thickness of 200 nm. Doses are in Gray and they are calculated assuming a X-ray flux equal to 1 mJ/cm^2 before the filters.

- (iii) the nucleus is made of 78% water and 22% biological material.

The cell average density is $\rho = 1.06 \text{ g/cm}^3$, comparable to the value reported by reference [11].

The doses absorbed by the three cell compartments are numerically computed using the Lambert-Bouguet-Beer law, that is the X-ray energy dE absorbed by a layer with thickness dx , density ρ and absorption coefficient μ is given by $dE/dx = -\mu\rho E$.

In this way it is possible to perform a simple study of the influence of the various parameters (compartment sizes, cell composition, radiation wavelength) on the absorbed dose.

Figure 6 shows the calculated doses for two values of X-ray energy ($h\nu \approx 0.9$ and 1.2 keV) for a cell with average dimension of the three compartments. The harder radiation is characterised by a much bigger energy deposition to the cell nucleus. Moreover the ratio between the dose to the wall and the dose to the nucleus is higher for the softer radiation.

In order to take into account the variation of the absorbed doses at $h\nu \approx 0.9 \text{ keV}$ due to the different sizes of the cells, calculations were performed for various values of the cell radius r_0 . In particular Figure 7 shows the doses to wall, cytoplasm and nucleus for different cell sizes. It is clear how the dose absorbed by the nucleus is high in cell, with a 2 μm radius which are likely to be found in the real cell suspension. Even for medium size cells, there is still a non-negligible absorption in the cell nucleus (Fig. 7), despite the fact that most of the energy is absorbed in the cell wall and in the cytoplasm.

Moreover, the emitted spectrum has several lines characterised by different absorption coefficients, the harder X-rays having a lower absorption coefficient and hence a longer penetration in biological material. This means that the higher energy lines travel through the cells with lower attenuation. Hence the X-ray spectrum becomes harder and harder while the radiation travels through the cells

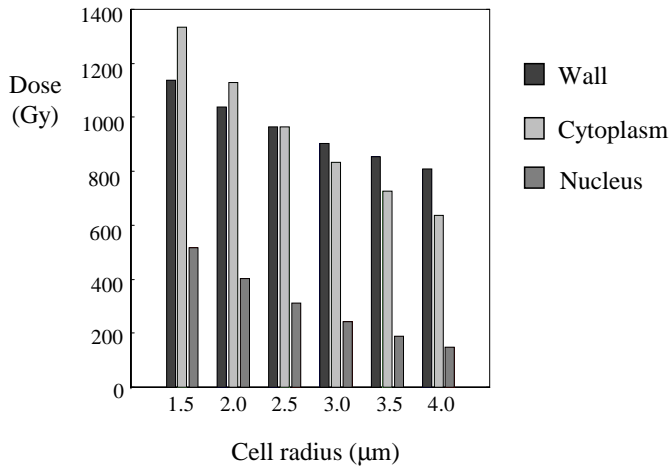


Fig. 7. Dosimetry of yeast cells as a function of cell radius calculated for 0.9 keV X-ray radiation and assuming an X-ray flux equal to 1 mJ/cm^2 before the filters. Wall thickness and nuclear radius change in a constant ratio.

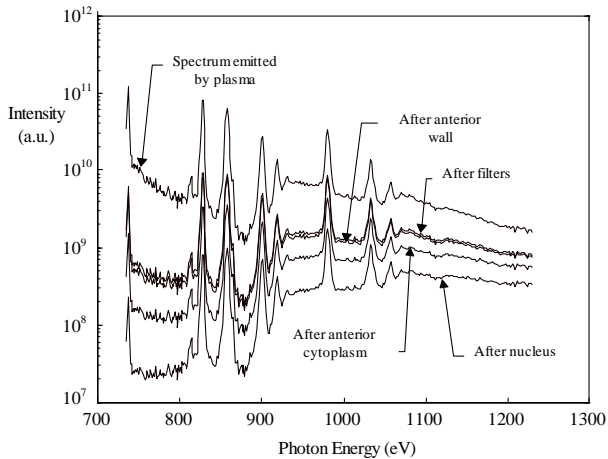


Fig. 8. Hardening effect on X-ray spectrum.

and the higher energy lines are more likely to deposit their energy in the cell nucleus. Such hardening effect is shown in Figure 8 as obtained from numerical processing of the measured spectrum.

This undesired effect was reduced by the insertion of a Cu filter ($0.2 \mu\text{m}$ thick) before the biological samples. As already said, the Cu *L*-shell absorption at 0.993 keV effectively removed most of the harder X-rays which are present in the CF_2 spectrum, so leading closer to the desired irradiation conditions. In following experiments some Neon will be added to the buffer gas contained in the interaction chamber. This will improve the irradiation conditions even more, being characterised by a *K*-edge absorption at 870 eV .

6 Experimental results

First, we analysed in detail CO_2 production *vs.* time on a very large amount of different samples. Figure 9 shows the

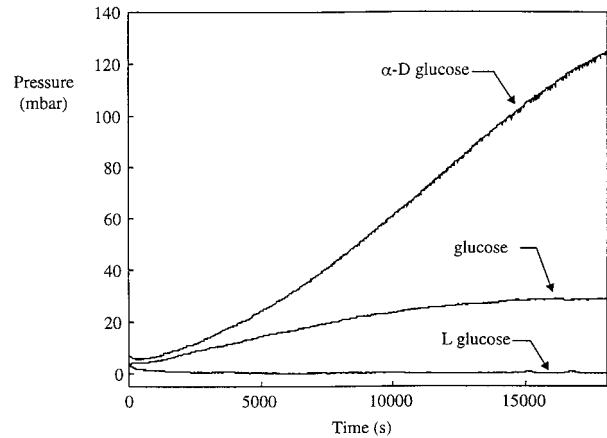


Fig. 9. CO_2 pressure measurements for samples fed with different kinds of sugar.

effects of the different sugars used in the sample suspensions on the cell metabolic activity which can be easily evidenced with our monitoring technique. The different rate of pressure increase shows the different cell capability of assuming different nutrients, *i.e.* *L*-glucose, glucose and αD -glucose (also *D*-mannose has been tested with an intermediate yield between glucose and αD -glucose). In particular no CO_2 pressure increase is visible for samples fed with *L*-glucose which has a chirality that does not allow this sugar to be metabolised. Moreover our technique has a sufficient sensitivity to different sugar compositions (like glucose and αD -glucose), with the αD -glucose being metabolised at a higher rate than other kinds of sugars.

This analysis has been performed in order to show that an accurate CO_2 pressure measurement is an efficient tool for the study of cell metabolic activity; moreover it is affordable, precise and reproducible. It is not the aim of this work to link these results to the available biological models for the fermentation, but obviously it can be a subject for further developments.

Some of the considered samples show evident oscillations in the pressure production. A spectral analysis of the time series has been done in order to extract the principal harmonic component of the signal. The signal has been preliminary detrended using a linear piecewise function; then Discrete Fourier transform is used in order to obtain the power spectrum (Fig. 10). In order to obtain smoother spectra, rejecting the noise in the measurement procedure, each signal has been convoluted with a suitable regular function which helps in obtaining more regular spectra. Both detrending and smoothing effects have been carefully investigated and taken into account [23,24]. For the non irradiated sample of Figure 10, a principal frequency component corresponding to a period of $35.7 \pm 2.5 \text{ s}$. Is clearly visible a very similar estimate of the oscillation period has been obtained from different samples; in all cases the considered samples were respectively 4 ml of a suspension with 20 mg/ml of αD -glucose and 2 mg/ml of yeast. Moreover such oscillations were not found in the simultaneously analysed control water. The evidence of the metabolic origin of the oscillation is even confirmed by

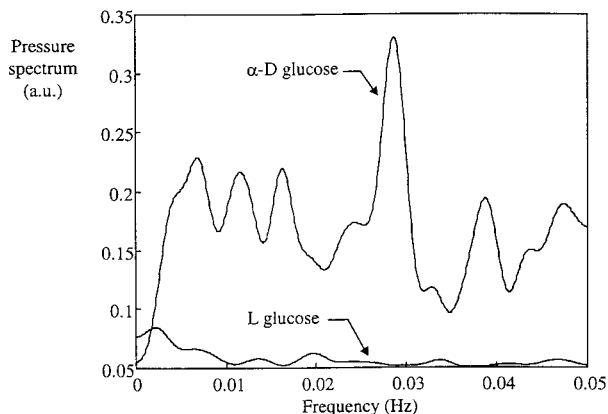


Fig. 10. Typical power spectra for two samples of standard cell suspension fed with α D-glucose and L-glucose respectively.

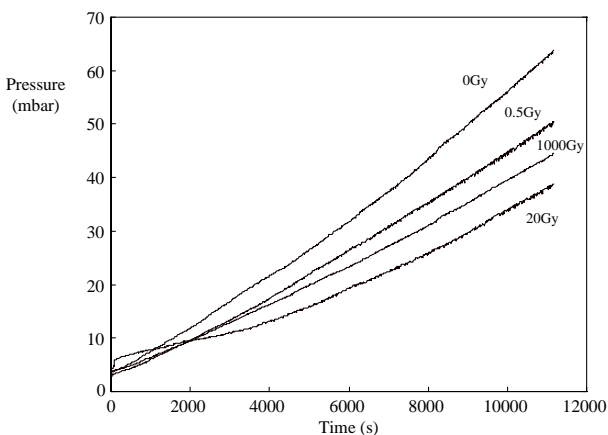


Fig. 11. CO₂ production as a function of time for various irradiation doses and for 4 ml of solution with 20 mg/ml of α D-glucose and 2 mg/ml of dry yeast cells.

the analysis of yeast cell suspension fed with L-glucose, in which we never observed any oscillatory phenomenon (*cf.* Fig. 10).

Later we analysed samples irradiated with different X-ray doses (between 0.5 and 1000 Gy). Typical results are shown in Figure 11. All the samples were fed with α D-glucose which enhanced the metabolic response as shown in Figure 9. A general CO₂ production rate decrease has been observed, together with a non-linear and non-monotone response to X-ray irradiation; this will be discussed in the following section.

Finally, oscillations were also observed and studied in irradiated samples. Figure 12 shows the frequency shifting and mixing as a consequence of irradiation. In this case the sample was again 4 ml of a solution of 20 mg/ml of α D-glucose and 2 mg/ml of yeast cells and were exposed with 20 Gy. The main frequency peak is shifted towards lower frequencies (giving now a main component period of 52.6 ± 5.5 s) and the rising of other frequency components is clearly visible. Such perturbations of spectra with frequency shifts and the appearance of various frequency components was registered in all the irradiated samples which exhibit oscillations. Anyway while the period of

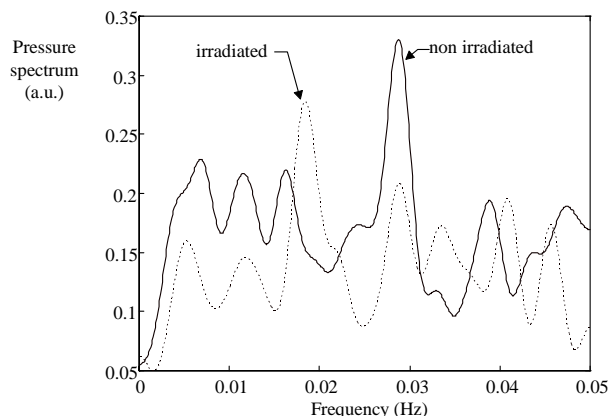


Fig. 12. Effect of radiation on CO₂ production. Comparison between the power spectra of a non irradiated cell suspension and a 20 Gy irradiated one; α D-glucose was used as nourishment in both suspensions.

about 36 s has been observed as greatly dominant in most non irradiated samples, in the case of irradiated cells no clear correlation between X-ray dose and the profile of the spectrum has been found for the moment. However, in general, since the main harmonic component moves towards lower frequencies, the metabolism of irradiated cells appear to occur at slightly lower rates, as confirmed also by the slower increase in CO₂ pressure (*cf.* Fig. 11). The appearance of many frequency could possibly be linked to the activation or exaltation of some less important glycolytic reactions, as already observed in [25].

7 Discussion

Let's start with the analysis of the behaviour of pressure *vs.* time. Figure 10 shows an initial phase of pressure increase, while later a saturation phase is approached. The initial phase is due to CO₂ accumulation inside the bottle while sugar is consumed and CO₂ is produced. Also some role can be played here by cell replication. Since the typical duplication time for *Saccharomyces cerevisiae* yeast cells is about 90 minutes [26] this process can indeed take place. However, in our case, the only nourishment given to the cells is sugar which assures the survivability of the cells but cannot give them all the elements which are needed for replication. Hence, very likely, our cells will undergo only one or a very few cellular duplication based on the use of their internal reserves, after which their number will become stationary, as we verified by cell counting at different times. The final saturation phase is instead connected to a reduction in metabolic activity in the fixed number of cells in the suspension. This is induced by the fact that, as time goes on, CO₂ (*i.e.* carbonic acid) and ethanol become more and more concentrated in the suspension and these have been observed to be important factors in reducing and finally arresting the cellular metabolic activity [27].

Often, after 2 to 3 hours, oscillations became evident in CO₂ production in some samples. Oscillations related

to metabolism have been previously observed in yeast extract [28] and in single yeast cells with other very invasive techniques [29,30]. Since we observe the phenomenon in yeast cell populations, a synchronisation mechanism must take place which correlates the different cells and phases them. Such mechanisms have already been described in literature; in particular in our case synchronisation can take place:

- (i) because of stress events imposed to the cells. In our experiments the sequence hydration, dehydration-irradiation-hydration is surely causing a stress to the cell and may produce an effective stress synchronisation mechanism, as realised in case of stress caused *i.e.* by thermal shocks [31,32];
- (ii) because the cells are undergoing starvation conditions [26,33,34]. In our case starvation is not related to sugar consumption (which is always in excess in the suspension), but it occurs because of the lack of other nutrient substances, as previously recalled speaking about cell replication.

The fact that a minimum time is required before the onset of the oscillations could possibly suggest a predominant role of the second mechanism (starvation synchronisation).

We think that there is a strict correlation between the observed metabolic oscillations and fermentation because:

- (i) CO₂ is produced by cells while O₂ is not consumed at the same rate, as confirmed by mass spectroscopy and by the fact that pressure in the bottles increases with time. Even if CO₂ can be soluted in water (forming carbonic acid) and cells can consume the O₂ initially dispersed in water, surely O₂ is less available to cells in the suspension than to cells exposed to air, suggesting almost anaerobic conditions. This also is probably due to the fact that the cells in the suspension tend quickly to deposit at the bottom of the bottle, thereby reducing the effective volume available per cell.
- (ii) As already recalled, an Argon atmosphere has sometimes been used inside the bottles in order to cause a further inhibition of respiration in favour of fermentation.
- (iii) Yeast cells often show a preference towards energy production *via* fermentation with respect to respiration [26,33]. This is especially true at high sugar concentration: when it is higher than 1 mg/ml it seems indeed to cause an inhibition of respiration [35] (we have used a 20 times bigger value).

If what observed is related to fermentation and oscillation in glycolytic cycle, then also the changes in CO₂ production and the frequency shift for irradiated cells must be connected to damages to the cell wall and cytoplasm, responsible for such activities. Moreover the dose calculation (*cf.* Sect. 5) seems to suggest that these compartments are those preferentially affected, even if damages to cell nuclear activity cannot be completely excluded.

Concerning CO₂ production rate *vs.* irradiation dose, we observed a non-linear and non-monotone mechanism

which is quite different from what is usually found in radiobiology experiment. The usual approach (for instance *cf.* Refs. [11,26]) is based on the study of survival curves, *i.e.* the capability of individual cells to develop colonies after the damage induced by X-rays. This only gives the response at very long times after irradiation, thereby losing all the information on fast cell response to damages and about cell damages which are not likely to be transmitted to the genetic descendants.

It is also worth to explicitly note the fact that the response is not connected to a simple saturation mechanism being non-monotone.

Even other techniques based on analyses at long times do not evidence such kind of response, even if they use different physical parameters to monitor cell reaction, as it happens with delayed luminescence [36].

This may suggest indications on transient effects and threshold repair mechanisms which may be activated at higher doses and remain inefficient at lower ones [37,38] and are at work at early times after irradiation. For instance X-ray irradiation has already been seen to induce transient effects in yeast cell membrane related to inhibition of enzymatic metabolic reaction [39].

The highlighting of such early response is possible thanks to the use of high brightness X-ray sources, like laser plasma, which allows to deliver large doses in a short time. This implies that cell reaction to the damaging factors does not start before the complete dose deposition: hence there are not changes in the biophysics of the studied process, as frequently happens in cell radiobiology.

8 Conclusion

In this paper we have studied cell metabolism by using a novel experimental technique based on pressure monitoring and X-ray irradiation. The use of very soft X-rays produced by a laser-plasma source gave the possibility to interfere with specific structures inside the cell (particularly wall), so that the changes of some peculiar mechanisms that take place in particular regions of the microorganisms can be analysed. We have developed a simple model for X-ray dosimetry which provides a quite clear and realistic picture of dose distribution inside the cells.

CO₂ measurement gave an evidence of metabolic oscillations. Oscillation frequency shifts, following exposure to soft X-rays, were observed, showing how this parameter can be important to understand the recovery processes in cells and the reactions after the induced damage.

Further research is now in progress in order to get a more reliable data statistics and improve the comprehension of the biophysical phenomena involved.

The experiment has been possible thanks to the Human Capital and Mobility “Access to Large Facilities” Programme, to INFN and to NATO (grant n. GRC961133). Special Thanks are due to: Cyril Brown, Anthony Parker, Colin Danson, Chris Edwards, Nick Allen, Katherine Hale, Irene Gray, Sue Tavenner, William Toner, Rick Allot, Nicola Lisi of RAL; to Roger

Brugge of the Meteo Dept Reading; to Rose Meldrum of the Biochemistry School, Birmingham; to David Stevens of MRC Harwell Laboratory; to Giampietro Braga, Giuliana Baroni and Lorenzo Ferraro of Dipartimento di Fisica (Milano); to Franco Cotelli and Carla Lora Lamia of Dipartimento di Biologia (Milano). A. Pozzi thanks the Italian Physical Society (SIF) and A. Masini the Istituto Nazionale di Fisica della Materia (INFN) for their grants.

References

1. M.F. Tuite, *Nature* **370**, 327 (1964).
2. E. Fremter, *Biophysics*, edited by W. Hoppe *et al.* (Springer-Verlag, Berlin, 1983).
3. A.T. Winfree, *The geometry of biological time* (Springer-Verlag, Berlin, 1983).
4. Voet and Voet, *Biochemistry* (Wiley & Sons Inc., New-York 1990).
5. P. Fantes, R. Brooks, *The cells cycle, a practical approach* (IRL Press, Oxford 1994).
6. S. Cortassa, M.A. Aon, *Cell Biol. Int.* **18**, 687 (1994).
7. G. Nicolis, I. Prigogine, *Self organisation in non equilibrium systems from dissipative structures to order through fluctuations* (Wiley & sons Inc., New-York, 1977).
8. E. Turcu, I. Ross, P. Trenda, M. Schulz, A.G. Michette, G. Tallents, D. Batani, C. Wharton, R. Meldrum *et al.*, in "Applications of Laser Plasma Radiation", San Diego (USA), SPIE Proc. **2015**, 243 (1994).
9. D. Batani, M. Milani, A. Masini, A. Pozzi, M. Costato, E. Turcu, N. Lisi, R. Allot *et al.*, *Physica Medica*, 1998 (in press).
10. F.M. Klis, *Yeast* **10**, 851 (1994).
11. D. Frankenberg, D.T. Goodhead *et al.*, *Int. J. Radiat. Biol.* **50**, 727 (1986).
12. J.N. Strathern *et al.*, *The molecular biology of yeast Saccharomyces*, (Cold Spring Laboratory, New York 1981).
13. D. Batani, M. Milani, A. Masini, F. Previdi, E. Turcu *et al.*, *Laser and Technology* **5**, 3 (1995).
14. E. Turcu, G.J. Tallents, I. Ross, A.G. Michette, M. Schulz, R.A. Meldrum, C.W. Wharton, D. Batani, M. Martinetti, A. Mauri, *Physica Medica* **10**, 93 (1994).
15. F. Bijkerk, E. Louis, M. van der Wiel, E. Turcu, G.J. Tallents, D. Batani, *J. X-ray Sci. Tech.* **3**, 133 (1992).
16. D. Batani, E. Turcu, G. Tallents, A. Giulietti, L. Palladino in "Excimer Lasers and Applications III", The Hague (The Netherlands), SPIE Proc. **1503**, 479 (1991).
17. P.D. Rockett, C.R. Bird, C.J. Hailey, D. Sullivan, D.B. Brown, P.G. Burkalter, *Appl. Opt.* **24**, 2536 (1985).
18. B.L. Henke, in *X-ray data booklet* Centre for X-ray optics, edited by D. Vaughan (Berkeley 1986).
19. N.G. Alexandropoulos, G.G. Cohen, *Appl. Spectr.* **28**, 2 (1974).
20. R.W. Lee, *User manual for Ration* (Lawrence Livermore National Laboratory 1990).
21. A. Magunov, A. Faenov, D. Batani, M. Milani, A. Conti, A. Masini, M. Costato, E. Turcu, M. Koenig, A. Benuzzi *et al.*, *Physica Scripta* **55**, 478 (1997).
22. R.C. Weast, M.J. Astle, *Handbook of Chemistry and Physics* (CRC Press, Boca Raton, 1983).
23. S. Bittanti, L. Piroddi, *J. Franklin Institute* **334**, 135 (1997).
24. T. Soderstrom, P. Stoica, *System identification*, Prentice Hall International, New Jersey (1989).
25. B. Hesse, *J. Exp. Biol.* **81**, (1979).
26. M.F. Tuite, S.G. Oliver, *Saccharomyces* (Plenum Press, New York, 1991).
27. M.A. Aon, S. Cortassa, H.V. Westerhoff, K. van Dam, *J. Gen. Microbiol.* **138** (1992).
28. A. Boiteux, A. Goldbeter, B. Hesse, *Proc. natn. Acad. Sci., USA* **72** (1975).
29. B. Chance, R.W. Estabrook, A. Ghosh, *Proc. natn. Acad. Sci., USA* **51** (1964).
30. A. Betz, *Quantitative biology and metabolism*, edited by A. Locker (Springer-Verlag, 1968).
31. I.L. Cameron, G.M. Padilla, *Cell Sincrony* (Academic Press, New York 1966).
32. A. Kockova-Kratochvilova, *Yeast and Yeast-like Organisms* (VCH, New York and Weinheim, 1990).
33. I. Lamprecht, *Biological microcalorimetry*, edited by A.E. Beezer (Academic Press, London, 1980).
34. A.E. Wheals, *The yeast*, edited by A.H. Rose, J.S. Harrison (Academic Press, London **1**, 1989).
35. P. Richard, C. Hogan, *Biotech. Bioing.* **20**, 1105 (1978).
36. D. Batani, A. Conti, A. Masini, M. Milani *et al.*, *Il Nuovo Cimento D* **18**, 657 (1996).
37. J. Calkins, M. Einspenner, E. Azzam, M. Kunhi, D. Sigut, M. Hannan, *Int. J. Radiat. Biol.* **59**, 1 (1991).
38. J. Calkins, E. Einspenner, W. Harrison, *Strahlen-therapie und Onkologie* **166**, (1990).
39. H. Rink, *Int. J. Radiat. Biol.* **27**, 305 (1975)